7-15-2011

Au nanospheres and nanorods for enzyme-free electrochemical biosensor applications

Yu-Ho Won
Purdue University, ywon@purdue.edu

Keon Huh
Purdue University, khuh@purdue.edu

Lia A. Stanciu
Purdue University, lstanciu@purdue.edu

Won, Yu-Ho; Huh, Keon; and Stanciu, Lia A., "Au nanospheres and nanorods for enzyme-free electrochemical biosensor applications" (2011). *Birck and NCN Publications.* Paper 755.
http://dx.doi.org/10.1016/j.bios.2011.05.012

Biosensors and Bioelectronics 26 (2011) 4514–4519

Contents lists available at ScienceDirect

Biosensors and Bioelectronics

journal homepage: www.elsevier.com/locate/bios

Au nanospheres and nanorods for enzyme-free electrochemical biosensor applications

Yu-Ho Won [a], Keon Huh [c], Lia A. Stanciu [a,b,*]

[a] School of Materials Engineering, Purdue University, West Lafayette, IN 47907, United States
[b] Birck Nanotechnology center, Purdue University, West Lafayette, IN 47907, United States
[c] School of Electrical and Computer Engineering, Purdue University, West Lafayette, IN 47907, United States

ARTICLE INFO

Article history:
Received 8 February 2011
Received in revised form 30 April 2011
Accepted 5 May 2011
Available online 12 May 2011

Keywords:
Au nanospheres
Nanorods
Biosensors
Electrocatalyst
Enzyme-free

ABSTRACT

Au nanocrystals with different morphologies were prepared and used for enzyme-free electrochemical biosensor applications. To investigate the electrocatalytic properties of Au nanocrystals as a function on their morphologies, Au nanocrystals, Au nanospheres (NSs) on silica, Au NSs, and Au nanorods (NRs) with aspect ratios of 1:3 and 1:5, were coated on the screen printed electrodes and further measure the amperometic responses to hydrogen peroxide via three-electrode system. The electrodes modified with Au nanocrystals showed biosensing properties without any enzyme being attached or immobilized at their surface. The hydrogen peroxide detection limits of the biosensors with Au NSs, Au NRs (1:3), and Au NRs (1:5) were 6.48, 8.65, and 9.38 μM (S/N = 3), respectively. The biosensors with Au NSs, Au NRs (1:3), and Au NRs (1:5) showed the sensitivities of 11.13, 54.53, and 58.51 μA/mM, respectively. These results indicate that morphologies of Au nanocrystals significantly influence the sensitivity of the biosensors. In addition, the enzyme-free biosensors with Au nanocrystals were stable for 2 months. Au nanocrystal-based enzyme-free system, which is proposed in this study, can be used as a platform for various electrochemical biosensors.

1. Introduction

Metal and semiconductor nanocrystals have been widely investigated in recent times due to their unique properties. Among several nanocrystals, Au nanocrystals have attracted intense attention since they have the potential to find several applications in fields such as catalysis (Liao et al., 2008), biosensing (Zhao et al., 2008; Singh et al., 2009; Beni et al., 2010; Chuang et al., 2010; Dondapati et al., 2010; Li et al., 2010; Lu et al., 2010; Zhang et al., 2010a), biological labeling (Lin et al., 2009). The physical, chemical, or catalytic properties of Au nanocrystals are dependent on their size and shape (Daniel and Astruc, 2004; Liao et al., 2008; Seo et al., 2008). Liao et al. (2008) demonstrated the fabrication of shape-controllable Au nanocrystals including snowflake, nanothorns, star-shaped particles and compared their electrocatalytic properties. Seo et al. (2008) reported characterization of optical properties of different shaped Au nanocrystals such as sphere, cube, and octahedron.

There are several approaches to test the biosensing capabilities of Au nanocrystals including the electrochemical method (Qin et al., 2010; Zhang et al., 2010a), inductively coupled plasma mass spectrometry (Li et al., 2010), colorimetry (Zhao et al., 2008; Lu et al., 2010) and two-photon scattering spectroscopy (Singh et al., 2009; Lu et al., 2010) that have been described in literature. These various approaches take advantage of the properties of Au nanocrystals such as surface plasmonic resonance, high conductivity, stability, biocompatibility, and efficient electrocatalytic properties (Bai et al., 2008b; Liao et al., 2008; Claussen et al., 2009). However, to the best of our knowledge, no systematic study was conducted on the influence of Au nanocrystals' morphologies on their biosensing characteristics as applied to the detection of hydrogen peroxide.

Biosensors have been developed for detection, quantification, and monitoring of specific biomolecules or chemical species for environmental, clinical, and industrial fields (Albareda-Sirvent et al., 2000; Lin et al., 2010). The accurate and efficient detection of hydrogen peroxide are significant for both biomedical and environmental fields. Hydrogen peroxide is produced through the reaction between glucose and glucose oxidase (GOD) in glucose biosensors (Claussen et al., 2009; Lin et al., 2010). In addition, high concentrations of hydrogen peroxide can have a negative effect on human health, provoking eyes and skin irritations (Lin et al., 2010; Won et al., 2010). Most of the electrochemical hydrogen peroxide biosensors are based on enzymes such as horseradish

* Corresponding author at: School of Materials Engineering, Purdue University, 701 West Stadium, West Lafayette, IN 47907-2045, United States.
Tel.: +1 765 496 3552; fax: +1 765 494 1204.
E-mail address: lstanciu@purdue.edu (L.A. Stanciu).

0956-5663/$ – see front matter © 2011 Elsevier B.V. All rights reserved.
doi:10.1016/j.bios.2011.05.012

peroxidase (HRP) with good results in terms of sensitivity and selectivity (Cai et al., 2006; Kafi et al., 2008; Won et al., 2010). However, enzyme-based biosensors have drawbacks, including a complex structure that increases cost, and poor stability because of the inherent nature of enzymes (Bai et al., 2008a,b; Lin et al., 2010; Zhang et al., 2010b). To overcome these drawbacks of enzyme-based biosensors, enzyme-free biosensors have been studied by using nanoparticle (NP)-modified electrodes or direct electrodes. Novel metal NPs (Pt, Pd, and Au), semiconductor NPs, and carbon nanotubes (CNTs) have been tested for use in the design of non-enzyme biosensors. Chakraborty and Raj (2009) reported on the fabrication of a Pt NS-based electrode for enzyme-free hydrogen peroxide detection. Lin et al. (2010) and Vlandas et al. (2010) demonstrated the design of enzyme-free amperometric biosensors by using CNTs. Zhang et al. (2009) and Wang et al. (2010) used Cu_2O and Cu–CuO nanowires to make enzyme-free glucose sensors. In addition, nanocomposites such as Pt–Pb nanowires (Bai et al., 2008a) and Pt–Pb alloy NPs/CNTs electrodes (Cui et al., 2006) were also investigated for their use in enzyme-free biosensors. As mentioned above, Au nanocrystals are good candidates for enzyme-free electrochemical biosensors since they have superior electrical conductivity, which holds the promise of fast electron transfer, a high surface area, and good electrocatalytic properties, important for achieving high sensitivity (Bai et al., 2008b; Liao et al., 2008; Claussen et al., 2009).

Herein, we present Au nanocrystal-based enzyme-free electrochemical biosensors for the detection of hydrogen peroxide. We based our work on the hypothesis that biosensors' performance could be potentially influenced by the morphologies of Au nanocrystals, which have different catalytic properties depending on their size and shape. To test this hypothesis, four types of Au nanocrystals including Au nanoshperes (NSs) on silica spheres, Au NSs, and Au nanorods (NRs) with aspect ratios of 1:3 and 1:5 were prepared and tested for their biosensing capability for the detection of hydrogen peroxide. As-prepared Au nanocrystals were coated on the screen printed electrode (SPE), which is a working electrode in a three-electrode system, and the amperometric responses of the SPEs to hydrogen peroxide were measured.

2. Experimental

2.1. Materials

In order to synthesize two types of Au NSs (Au NSs on silica and Au NSs), $HAuCl_4$, $NaBH_4$, polyvinyl pyrrolidone (PVP), tetraethyl orthosilicate (TEOS), ammonium hydroxide, 2-propanol, and ethanol were purchased from Sigma Aldrich. Au NRs, dispersed in deionized (DI) water with 0.1% ascorbic acid and <0.1% cetyl trimethylammonium bromide (CTAB) surfactant capping agents, were purchased from Nanopartz (model #: 30-10-780 and 30-10-850). Hydrogen peroxide (H_2O_2, 30%, w/v solution), $K_4Fe(CN)_6$, and $K_3Fe(CN)_6$ were purchased from Sigma Aldrich for the hydrogen peroxide biosensor tests. KH_2PO_4, and K_2HPO_4, and KCl were obtained from Sigma Aldrich for the preparation of the phosphate buffer solution (PBS).

2.2. Synthesis of Au nanocrystals

To prepare Au NS-decorated silica spheres, monodispersed silica spheres were synthesized by the Stöber method which uses the hydrolysis and condensation of sol–gel precursor (Stöber et al., 1968). TEOS as a precursor and ammonium hydroxide as a catalyst were reacted in 2-propanol solution. As-synthesized silica spheres were washed several times and re-dispersed in DI water. Then, Au NSs were formed on the silica spheres via the modified approach of Kamat group (Dawson and Kamat, 2000). $HAuCl_4$ solution (2.5 mM, 100 μl) was added to the silica solution (100 μl) while the solution was stirred. Freshly prepared 10 μl of $NaBH_4$ solution (0.03 wt%) is added to the mixed solution for the reduction of $[AuCl_4]^-$. Then, the solution was washed to remove unreactants.

Au NSs were synthesized via the method which was reported by Lim et al. (2008) $HAuCl_4$ solution (0.05 mM) was prepared and fast injected into the PVP solution (10 mg in 10 ml DI water) at 100 °C. The mixed solution was heated at the same temperature for 1 h and then cooled to 25 °C. Then, the solution was washed to remove excessive PVP and re-dispersed in DI water.

2.3. Apparatus and measurements

Transmission electron microscopy (TEM) images of Au nanocrystals were obtained using a Tecnai 20 (FEI) operating at 200 kV. The ultraviolet visible (UV–Vis) absorption spectra were recorded using a SpectraMax M5 spectrometer (Molecular Devices). The electrochemical measurements of the biosensors for the detection of hydrogen peroxide were performed with a BASi epsilon C3 cell stand. A conventional three-electrode system, which consists of screen printed electrode (SPE; area = 4 mm × 5 mm, Pine Research Instrumentation) as a working electrode, Pt wire as a counter electrode, and Ag/AgCl electrode as a reference electrode, was used for the biosensor measurements.

2.4. Preparation and characterization of the biosensors

Au nanocrystal-based enzyme-free biosensors were simply fabricated by coating Au nanocrystals on SPEs. Au nanocrystals dispersed in DI water were dropped on the surface of SPEs (area = 4 mm × 5 mm) which were pre-treated to render their surface hydrophilic and dried for 2 h at 25 °C. Au nanocrystals are attached to the surface of the SPE by physical interaction. Usually, nano-sized particles tend to attach well to surfaces of SPEs in their attempt to reduce their surface energy. PBS solution (0.05 M, pH 7) containing KH_2PO_4 and K_2HPO_4 was prepared and its pH values were adjusted to be from 4 to 7 using HCl. Amperometric responses of the biosensors were obtained in 3 ml PBS (0.05 M, pH 7) containing 10 mM $[Fe(CN)_6]^{3-/4-}$, under magnetic stirring (150 rpm) at an applied potential of 200 mV.

3. Results and discussion

3.1. Preparation and characterization of Au Nanocrystals

Au NSs and Au NRs were prepared for the comparison of the biosensors properties depending on morphologies of Au nanocrystals. Fig. 1(a1–a3) shows a schematic, a transmission electron microscopy (TEM) image, and an ultraviolet–visible (UV–Vis) spectrum of Au NS-decorated silica spheres. Au NSs were deposited on silica spheres (100 nm in diameter), which were separately synthesized by the Stöber method (Stöber et al., 1968) via reduction of $[AuCl_4]^-$ by freshly prepared $NaBH_4$ solution (Dawson and Kamat, 2000). The size of Au NSs ranges from 7 to 20 nm and the surface plasmon resonance (SPR) peak of Au NSs on silica appeared at 535 nm. Au NSs were synthesized via the method reported by Lim et al. (2008). Only the synthesis method used by Lim et al. to synthesize Au NSs was used in our work, although this paper reported the synthesis of other Au nanostructures. Our results showed that the size of synthesized Au NSs varied in the range of 10–40 nm and the SPR peak showed at 540 nm, as shown in Fig. 1(b1–b3). Most of Au NSs are nearly spherical and a few Au NSs are irregular. We therefore believe it is reasonable to refer to these structures as Au NS. Moreover, although there are a few Au NSs with irregular shape, they are equiaxed. Prepared Au NRs have two different

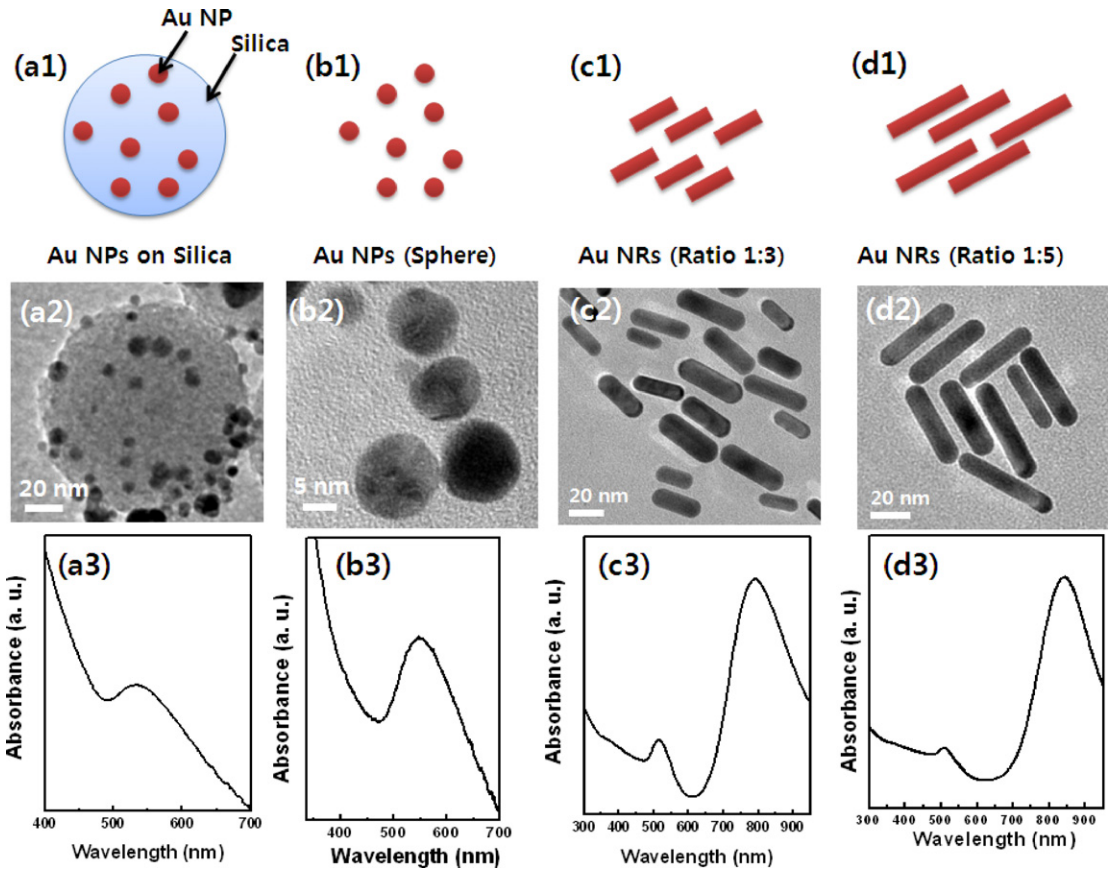

Fig. 1. (a) Au NSs on silica, (b) Au NSs, (c) Au NRs (ratio 1:3), and (d) Au NRs (ratio 1:5). (1)–(3) are a schematic, a TEM image, and an UV–Vis spectrum, respectively.

aspect ratios, which are 1:3 and 1:5 with 10 nm along short axis and 30 and 50 nm along long axis, respectively (Fig. 1(c2 and d2)). Two different SPR peaks in each UV–Vis absorption spectrum were observed in visible spectral region, corresponding to transverse and longitudinal surface plasmon modes for Au NRs (Fig. 1(c3 and d3)). Au NRs with aspect ratios of 1:3 and 1:5 have transverse SPR peaks at 515 and 510 nm and longitudinal SPR peaks at 790 and 850 nm, respectively. The transverse SPR bands showed a slight blue shift, while the longitudinal SPR bands shifted to a significantly longer wavelength as the aspect ratio of Au NRs increased. These results are in good agreement with previously published data (Song et al., 2005).

3.2. *Au nanocrystal-based enzyme-free biosensor*

Following preparation of Au nanocrystals of different morphologies, enzyme-free electrochemical biosensors for the detection of hydrogen peroxide were fabricated. The SPEs were used as a working electrode in a three-electrode setup. Au nanocrystals were coated on the surface of SPEs and dried for 2 h, as shown in Fig. 2. Then, the biosensors were electrochemically tested in 3 ml of phosphate buffer solution (PBS, 0.05 M, pH 7) containing 10 mM $[Fe(CN)_6]^{3-/4-}$, which are electron mediators. Hydrogen peroxide (H_2O_2) is reduced to H_2O, while $Fe(CN)_6^{4-}$ is oxidized to $Fe(CN)_6^{3-}$. The electrons that are produced from the reduction of $Fe(CN)_6^{3-}$ to

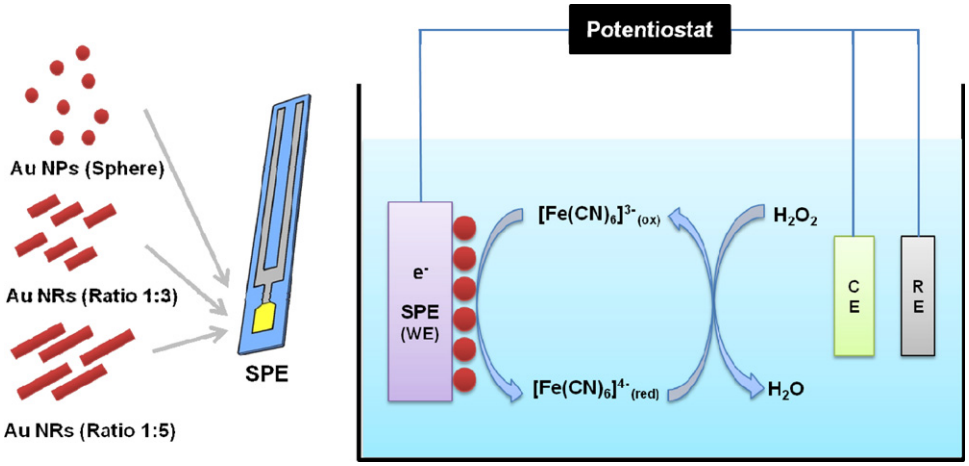

Fig. 2. Schematic of enzyme-free hydrogen peroxide biosensor and the reaction on the electrode (SPE: screen printed electrode, WE: working electrode, CE: counter electrode, RE: reference electrode).

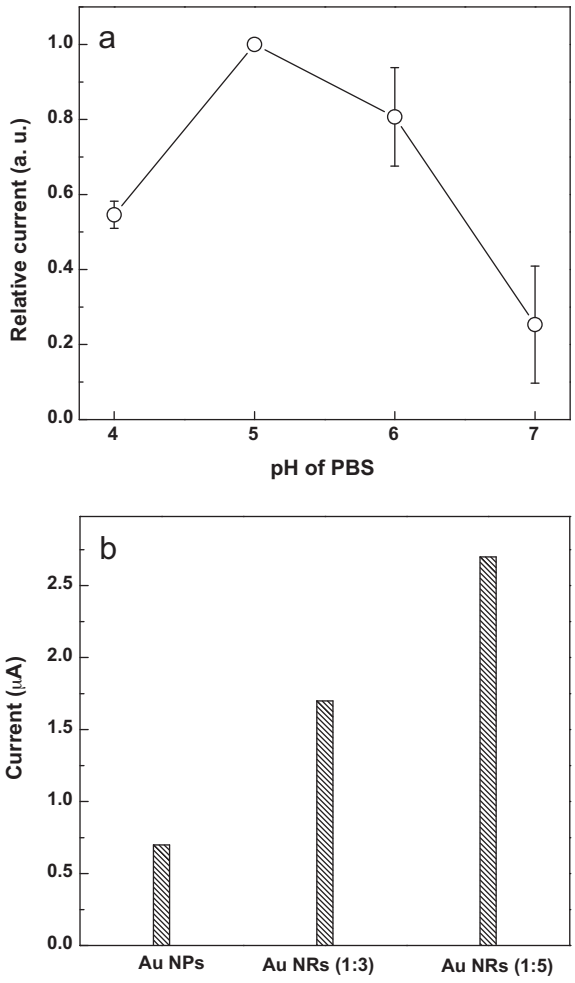

Fig. 3. Amperometric responses of (a) the biosensor with Au NSs to various pH values of PBS (0.05 M) containing 10 mM $[Fe(CN)_6]^{3-/4-}$ at 200 mV to 0.33 mM hydrogen peroxide, (b) the biosensors with Au NSs, Au NRs (1:3), and Au NRs (1:5) in the PBS (0.05 M, pH 5) containing 10 mM $[Fe(CN)_6]^{3-/4-}$ at 200 mV to 0.33 mM hydrogen peroxide.

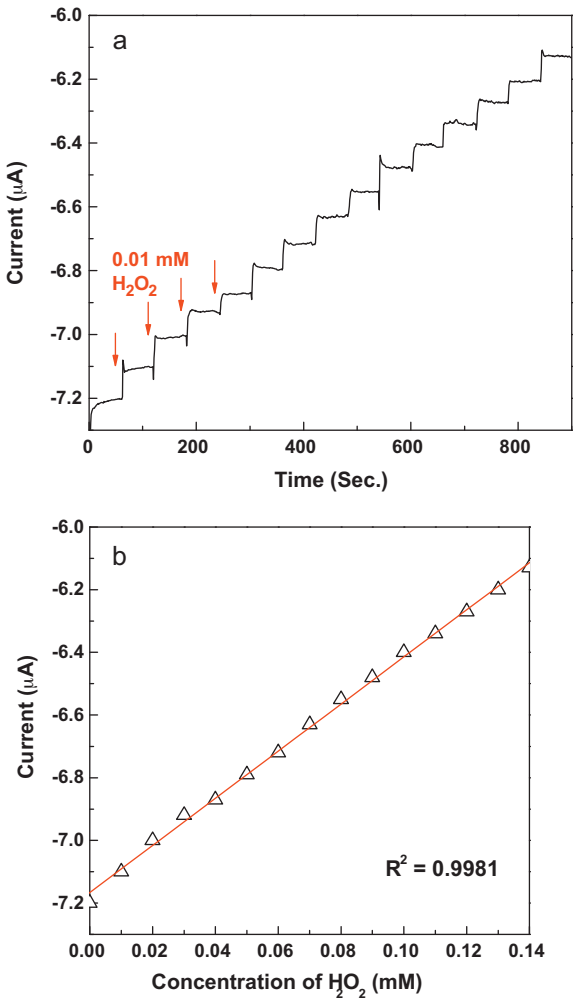

Fig. 4. Amperometric response of Au NS-based enzyme-free biosensors for the detection of hydrogen peroxide (a) response in PBS (0.05 M, pH 5) containing 5 mM $[Fe(CN)_6]^{3-/4-}$ at an applied potential of 200 mV with successive additions of 0.01 mM hydrogen peroxide (b) calibration plot (current vs. concentration of hydrogen peroxide) with linear regression analysis.

$Fe(CN)_6^{4-}$ are moved to the SPE through Au nanocrystals (Fig. 2). The concentration of hydrogen peroxide can be detected based on the fact that it is proportional to the current response. Surprisingly, the biosensor constructed based on Au NSs on silica showed no redox current response with the reduction of hydrogen peroxide in the preliminary tests. This may the effect of the lower electrical conductivity of the silica, which acted as a barrier to the movement of electrons to the SPE. This effect indicates that the conductivity of electrocatalytic materials is paramount for their ability to serve as a platform for the design of enzyme-free biosensors. The biosensor designed with Au NSs on silica was therefore not taken into consideration when the performance of Au nanocrystals with various morphologies was compared in terms of their potential to be used in hydrogen peroxide biosensors.

The biosensor properties are affected by the pH value of buffer solution, the applied potential, and the concentration of the electron mediator, $[Fe(CN)_6]^{3-/4-}$. To optimize the measurement conditions, the amperometric responses were measured under various values of parameters such as the pH value of PBS, applied potential, and concentration of electron mediator. The current response showed the maximum value at an applied potential of 200 mV. Fig. 3(a) shows amperometric responses of the Au NS-modified electrode with various pH values of PBS at an applied potential of 200 mV. The current response reached the highest value in the PBS of pH 5. Thus, these conditions (PBS of pH 5 and an applied potential of 200 mV) were used for the subsequent biosensor tests.

Fig. 3(b) shows how the biosensor properties are influenced by the morphologies of Au nanocrystals. The amperometric responses were measured at the optimum conditions when 0.33 mM hydrogen peroxide was added into PBS (0.05 M, pH 5). The SPEs with Au NSs, Au NRs (1:3), and Au NRs (1:5) showed current responses of 0.7, 1.7, and 2.7 μA, respectively. The biosensors based on Au NRs showed a higher sensitivity than the biosensor employing Au NSs. Although the inherent resolution limitation of the SEM characterization of Au nanocrystal coated electrodes (see Supporting information) prevents us for making a statement of the true reasons behind these results, we can speculate on the possible effect of the Au nanocrystal morphology (NSs vs. NRs) on the electron transfer ability between these nanocrystals and the SPEs. The SPE with Au NRs may have a better electronic continuity because of a smaller number of interfacial boundaries between the NRs, when compared with a higher number of such boundaries for the NSs. In turn, this could have an effect on the electron transfer rate of the SPE with Au NRs being higher compared with the SPE with Au NSs. These results are in good agreement with the report of Zhang et al. (2010b) in which the authors showed that the electron transfer resistance of CuO NSs is larger than that of CuO nanowires in

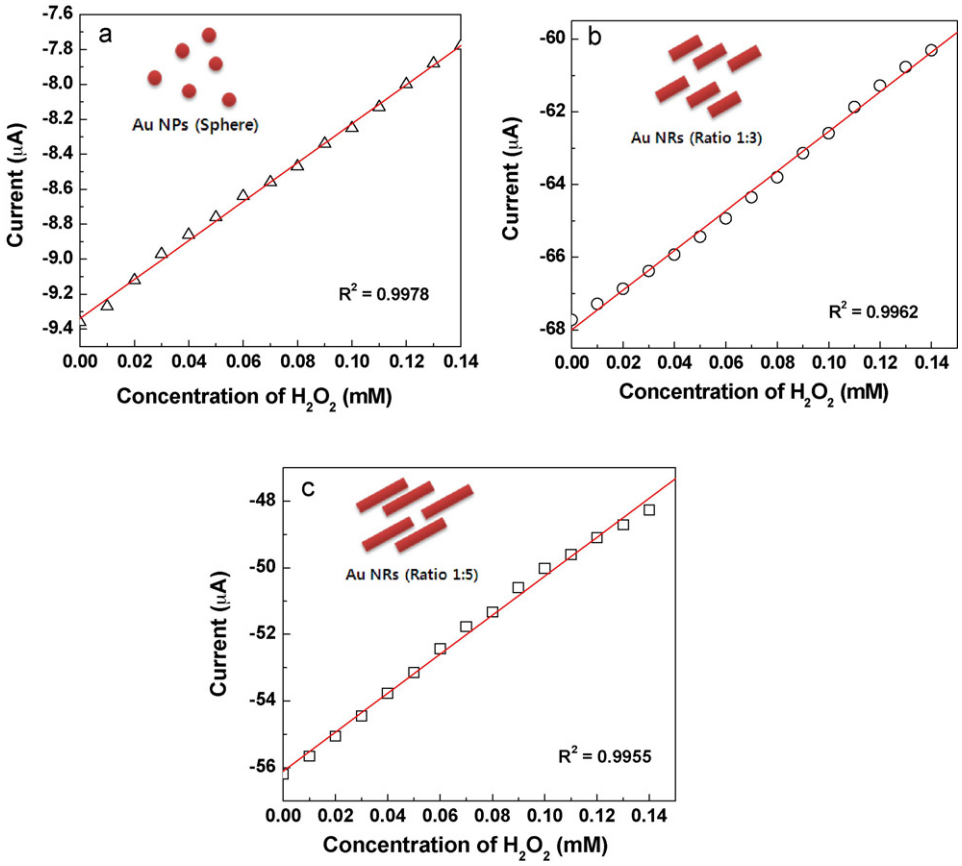

Fig. 5. Amperometric responses of enzyme-free biosensors for the detection of hydrogen peroxide in PBS (0.05 M, pH 5) containing 10 mM $[Fe(CN)_6]^{3-/4-}$ at an applied potential of 200 mV with successive additions of 0.01 mM hydrogen peroxide. (a) Au NS-based, (b) Au NR (1:3)-based, and (c) Au NR (1:5)-based biosensors, separately.

enzyme-free biosensors. In addition, Au NRs (1:5) showed higher current response than Au NRs (1:3). This shows that a high aspect ratio in the Au nanocrystals leads to a biosensor design with a higher sensitivity.

To evaluate the properties of the Au nanocrystal-based enzyme-free biosensor, the amperometric currents were measured while 0.01 mM hydrogen peroxide was added successively into PBS (0.05 M, pH 5) containing 5 mM $[Fe(CN)_6]^{3-/4-}$ at 200 mV. As shown in Fig. 4(a), the electrode with Au NSs exhibited increase in current associated with successive addition of hydrogen peroxide. Fig. 4(b) shows calibration plot with linear regression analysis for current vs. concentration of hydrogen peroxide. The current responses have linear relationship with the concentration of hydrogen peroxide. The detection limit was calculated to be 6.05 μM hydrogen peroxide (signal to noise = 3) and the sensitivity was 7.52 μA/mM.

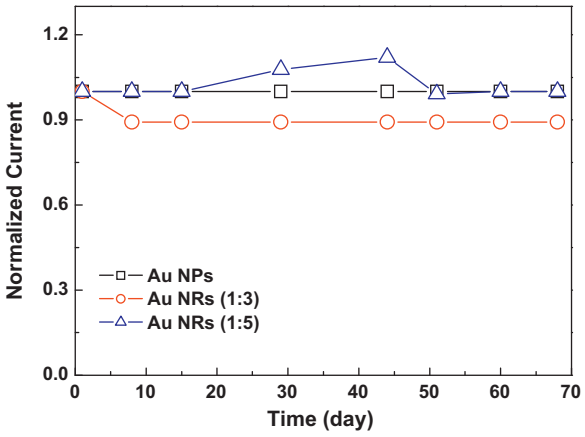

Fig. 6. Stability test of Au nanocrystal-based enzyme-free biosensors over 68 days in the PBS (0.05 M, pH 5) containing 10 mM $[Fe(CN)_6]^{3-/4-}$ at 200 mV to 0.33 mM hydrogen peroxide.

Fig. 5 shows amperometric response of SPE with Au NSs, Au NRs (1:3), and Au NRs (1:5) with successive additions of hydrogen peroxide of 0.01 mM. These calibration curves are plotted by the current response with time as shown in Fig. S2 (Supporting information). The effect of the concentration of electron mediator was investigated. Fig. 5(a) shows the amperometric response of the biosensor with Au NSs in PBS (0.05 M, pH 5) containing 10 mM $[Fe(CN)_6]^{3-/4-}$ at 200 mV. The current response is proportional to the hydrogen peroxide concentration. Hydrogen peroxide detection limit was estimated to be 6.48 μM (signal to noise = 3) and the sensitivity was 11.13 μA/mM. The sensitivity of the biosensor with Au NSs was improved by about 48% in the PBS containing 10 mM $[Fe(CN)_6]^{3-/4-}$ compared with that in the PBS containing 5 mM $[Fe(CN)_6]^{3-/4-}$. Thus, the biosensors based on Au NRs were tested in a PBS containing 10 mM $[Fe(CN)_6]^{3-/4-}$, since the sensitivity of the biosensor was improved under these conditions while maintaining a similar detection limit to the biosensor tested in a PBS containing 5 mM $[Fe(CN)_6]^{3-/4-}$. Fig. 5(b and c) shows current responses of biosensors fabricated with Au NRs (1:3) and (1:5), respectively, in PBS (0.05 M, pH 5) containing 10 mM $[Fe(CN)_6]^{3-/4-}$ at 200 mV with successive additions of 0.01 mM hydrogen peroxide. The biosensors with Au NRs showed linear relationship between currents and concentrations of hydrogen peroxide in the same as the biosensor with Au NSs. The detection limits of the biosensors with Au NRs (1:3) and (1:5) were 8.65 and 9.38 μM hydrogen peroxide (signal to noise = 3), respectively. The sensitivities of the biosensors with Au NRs (1:3) and (1:5) were 54.53 and 58.51 μA/mM, respectively. This indicates that the sensitivity of Au nanocrystal-based

enzyme-free biosensors strongly depends on morphologies of Au nanocrystals. However, the detection limits of hydrogen peroxide were not significantly changed regardless of morphologies of Au nanocrystals.

3.3. Stability of the biosensors

The stability in time of each of the Au nanocrystal-based enzyme-free biosensors was investigated. The electrodes were stored in air at 4 °C and the current response was periodically measured. Fig. 6 shows the current responses of three types of biosensors for 68 days. The current responses were measured under the same conditions, i.e. PBS (0.05 M, pH 5) containing 10 mM $[Fe(CN)_6]^{3-/4-}$ at 200 mV to 0.33 mM hydrogen peroxide. The current responses showed more than 90% retention of the initial values irrespective of morphologies of Au nanocrystals.

4. Conclusion

In conclusion, Au nanocrystal-based enzyme-free biosensors for the detection of hydrogen peroxide were prepared. To investigate the electrocatalytic properties depending on morphologies of Au nanocrystals such as Au NSs on silica spheres, Au NSs, and Au NRs with aspect ratios of 1:3 and 1:5 were prepared and characterized. The biosensors were fabricated simply by coating Au nanocrystals on the surface of SPE, a working electrode. The biosensors efficiently sensed successive increases of hydrogen peroxide except the biosensor with Au NSs on silica because of the poor conductivity of silica. Amperometric responses of biosensors with Au NSs, Au NRs (1:3), and Au NRs (1:5) demonstrated similar performances in terms of hydrogen peroxide detection limit and linear range. On the other hand, the sensitivity of the biosensors was significantly influenced by morphologies of Au nanocrystals. The Au NRs (1:5) coated electrode showed the highest sensitivity because of the highest electronic continuity of Au NRs with high aspect ratio. Au nanocrystal-based enzyme-free biosensor, displaying low detection limit, high sensitivity, and good stability, is promising as a platform for various biosensors. The effects of morphologies of Au nanocrystals could be used to tailor the fabrication of biosensors with desired characteristics.

Acknowledgements

The authors are grateful for the financial support provided by NSF DMR #0804464 and NSF OISE#0728130 awards

Appendix A. Supplementary data

Supplementary data associated with this article can be found, in the online version, at doi:10.1016/j.bios.2011.05.012.

References

Albareda-Sirvent, M., Merkoci, A., Alegret, S., 2000. Sens. Actuators B: Chem. 69, 153–163.
Bai, Y., Sun, Y.Y., Sun, C.Q., 2008a. Biosens. Bioelectron. 24, 579–585.
Bai, Y., Yang, W.W., Sun, Y., Sun, C.Q., 2008b. Sens. Actuators B: Chem. 134, 471–476.
Beni, V., Hayes, K., Lerga, T.M., O'Sullivan, C.K., 2010. Biosens. Bioelectron. 26, 307–313.
Cai, W.Y., Xu, Q., Zhao, X.N., Zhu, J.H., Chen, H.Y., 2006. Chem. Mater. 18, 279–284.
Chakraborty, S., Raj, C.R., 2009. Biosens. Bioelectron. 24, 3264–3268.
Chuang, Y.C., Li, J.C., Chen, S.H., Liu, T.Y., Kuo, C.H., Huang, W.T., Lin, C.S., 2010. Biomaterials 31, 6087–6095.
Claussen, J.C., Franklin, A.D., ul Haque, A., Porterfield, D.M., Fisher, T.S., 2009. ACS Nano 3, 37–44.
Cui, H.F., Ye, J.S., Liu, X., Zhang, W.D., 2006. Nanotechnology 17, 2334–2339.
Daniel, M.C., Astruc, D., 2004. Chem. Rev. 104, 293–346.
Dawson, A., Kamat, P.V., 2000. J. Phys. Chem. B 104, 11842–11846.
Dondapati, S.K., Sau, T.K., Hrelescu, C., Klar, T.A., Stefani, F.D., Feldmann, J., 2010. ACS Nano 4, 6318–6322.
Kafi, A.K.M., Wu, G., Chen, A., 2008. Biosens. Bioelectron. 24, 566–571.
Li, F., Zhao, Q., Wang, C.A., Lu, X.F., Li, X.F., Le, X.C., 2010. Anal. Chem. 82, 3399–3403.
Liao, H.G., Jiang, Y.X., Zhou, Z.Y., Chen, S.P., Sun, S.G., 2008. Angew. Chem. Int. Ed. 47, 9100–9103.
Lim, B., Camargo, P.H.C., Xia, Y.N., 2008. Langmuir 24, 10437–10442.
Lin, C.A.J., Yang, T.Y., Lee, C.H., Huang, S.H., Sperling, R.A., Zanella, M., Li, J.K., Shen, J.L., Wang, H.H., Yeh, H.I., Parak, W.J., Chang, W.H., 2009. ACS Nano 3, 395–401.
Lin, K.C., Tsai, T.H., Chen, S.M., 2010. Biosens. Bioelectron. 26, 608–614.
Lu, W.T., Arumugam, R., Senapati, D., Singh, A.K., Arbneshi, T., Khan, S.A., Yu, H.T., Ray, P.C., 2010. ACS Nano 4, 1739–1749.
Qin, X., Wang, H.C., Wang, X.S., Miao, Z.Y., Chen, L.L., Zhao, W., Shan, M.M., Chen, Q.A., 2010. Sens. Actuators B: Chem. 147, 593–598.
Seo, D., Yoo, C.I., Park, J.C., Park, S.M., Ryu, S., Song, H., 2008. Angew. Chem. Int. Ed. 47, 763–767.
Singh, A.K., Senapati, D., Wang, S.G., Griffin, J., Neely, A., Candice, P., Naylor, K.M., Varisli, B., Kalluri, J.R., Ray, P.C., 2009. ACS Nano 3, 1906–1912.
Song, J.H., Kim, F., Kim, D., Yang, P.D., 2005. Chem. Eur. J. 11, 910–916.
Stöber, W., Fink, A., Bohn, E., 1968. J. Colloid. Interface Sci. 26 (62).
Vlandas, A., Kurkina, T., Ahmad, A., Kern, K., Balasubramanian, K., 2010. Anal. Chem. 82, 6090–6097.
Wang, G.F., Wei, Y., Zhang, W., Zhang, X.J., Fang, B., Wang, L., 2010. Microchim. Acta 168, 87–92.
Won, Y.H., Aboagye, D., Jang, H.S., Jitianu, A., Stanciu, L.A., 2010. J. Mater. Chem. 20, 5030–5034.
Zhang, T.J., Wang, W., Zhang, D.Y., Zhang, X.X., Ma, Y.R., Zhou, Y.L., Qi, L.M., 2010a. Adv. Funct. Mater. 20, 1152–1160.
Zhang, X.J., Gu, A.X., Wang, G.F., Wei, Y., Wang, W., Wu, H.Q., Fang, B., 2010b. Crystengcomm 12, 1120–1126.
Zhang, X.J., Wang, G.F., Zhang, W., Wei, Y., Fang, B., 2009. Biosens. Bioelectron. 24, 3395–3398.
Zhao, W.A., Ali, M.M., Aguirre, S.D., Brook, M.A., Li, Y.F., 2008. Anal. Chem. 80, 8431–8437.